Phonon anharmonicity of monoclinic zirconia and yttrium-stabilized zirconia

C. W. Li, H. L. Smith, T. Lan, J. L. Niedziela, J. A. Muñoz, J. B. Keith, L. Mauger, D. L. Abernathy, and B. Fultz

Phys. Rev. B **91**, 144302 — Published 13 April 2015

DOI: 10.1103/PhysRevB.91.144302

Phonon Anharmonicity of Monoclinic Zirconia and Yttrium-Stabilized Zirconia

C. W. Li,[1,2,*] H. L. Smith,[2] T. Lan,[2] J. L. Niedziela,[3] J. A. Muñoz,[2]
J. B. Keith,[2] L. Mauger,[2] D. L. Abernathy,[4] and B. Fultz[2]

[1] *Materials Science and Technology Division, Oak Ridge National Laboratory, Oak Ridge, Tennessee, 37831*
[2] *Department of Applied Physics and Materials Science, California Institute of Technology, Pasadena, California, 91125*
[3] *Instrument and Source Division, Oak Ridge National Laboratory, Oak Ridge, Tennessee, 37831*
[4] *Quantum Condensed Matter Division, Oak Ridge National Laboratory, Oak Ridge, Tennessee, 37831*

Inelastic neutron scattering measurements on monoclinic zirconia (ZrO_2) and 8 mol% yttrium-stabilized zirconia were performed at temperatures from 300 to 1373 K. Temperature-dependent phonon densities of states (DOS) are reported, as are Raman spectra obtained at elevated temperatures. First-principles lattice dynamics calculations with density functional theory gave total and partial phonon DOS curves, and mode Grüneisen parameters. These mode Grüneisen parameters were used to predict the experimental temperature dependence of the phonon DOS, with partial success. However, substantial anharmonicity was found at elevated temperatures, especially for phonon modes dominated by the motions of oxygen atoms. Yttrium-stabilized zirconia (YSZ) was somewhat more anharmonic, and had a broader phonon spectrum at low temperatures, owing in part to defects in its structure. YSZ also has a larger vibrational entropy than monoclinic zirconia.

PACS numbers: 63.20.-e, 63.20.Ry, 63.20.D-, 77.84.Bw, 78.20.Bh, 78.70.Nx

I. INTRODUCTION

Zirconia (ZrO_2) is the most common and stable compound of zirconium found in nature, and one of the most studied ceramic materials. Zirconia is monoclinic ($P2_1c$, baddeleyite) at ambient pressure and temperature, transforms to a tetragonal phase ($P4_2nmc$) at approximately 2000 K,[1,2] and to a cubic phase ($Fm3m$, which differs sightly from the tetragonal phase by displacements of oxygen atoms) at higher temperatures and pressures.[1] The high temperature phases of ZrO_2 can be stabilized at ambient temperature and pressure by substituting some magnesium, calcium, cerium, or yttrium in place of zirconium to produce "stabilized zirconia". In particular, 8 mol% yttrium-stabilized zirconia (YSZ), which is a composition of technological importance, primarily takes the tetragonal phase. This YSZ has about 4% oxygen vacancies, consistent with valences of Y^{3+} and Zr^{4+}.

Zirconium-based oxides are leading candidates to replace silicon oxide as gate insulators in field effect transistors,[3,4] and their chemical stability and physical hardness also make them useful as optical coatings. YSZ has applications in solid oxide fuel cells because of high ionic conductivity owing to ion hopping at temperatures near or above 800 K.[5] Zirconia and YSZ both have high bulk moduli and high melting temperatures, making them important materials for high temperature applications.[6] YSZ is also one of the most widely-used materials for thermal barrier coatings, owing to its property of transformation toughening and its surprisingly low thermal conductivity of about $2\,W/(m \cdot K)$, which is much lower than the monoclinic phase.[7] The oxygen vacancies in YSZ are believed to have a major effect on thermal transport, but their interactions with phonons are not understood.

A contribution to the heat capacity at constant pressure is expected as the crystal expands against its bulk modulus. "Quasiharmonic" shifts of phonon frequencies arise because phonon frequencies usually decrease in an expanded crystal, giving an increased vibrational entropy. In the quasiharmonic approximation (QHA), it is assumed that the phonon modes are harmonic and non-interacting, but with shifted frequencies. Anharmonic effects arise from phonon-phonon interactions, which are caused by cubic or quartic terms in the phonon potential. Non-harmonic effects are important for understanding thermodynamic stability and thermal transport properties at elevated temperature,[8] but only a few studies of phonons in metal oxides at high temperatures have been reported. Anharmonicity in beryllia has been attributed to a change of phonon lifetime resulting from phonon-phonon interactions.[9] Phonon lifetime calculations on MgO showed anharmonicity at high pressures and temperatures.[10] Anharmonicity in cuprite Ag_2O was explained by the phonon-phonon interactions between Ag and O dominated modes, and this anharmonicity contributed to the negative thermal expansion.[11]

Vibrational spectroscopy studies and theoretical work on zirconia have been performed,[1,12–15] and other studies were focused on phase transitions under pressure.[16–18] In recent studies of the phonon dynamics of hafnia and zirconia, we reported measurements of Raman line positions and shapes to temperatures of about 1000 K, and correlated anharmonic effects to the vibrational displacements of oxygen atoms in the unit cell.[19,20] Similar work on YSZ showed an unexpectedly large softening in one of the phonon modes, and a large thermal broadening of Raman-active modes.[21] Cubic YSZ is also known to have large thermal parameters and Debye-Waller factors.[22] Some phonon dispersion curves were measured with triple-axis neutron spectrometry on cubic YSZ. The longitudinal and transverse acoustic phonon

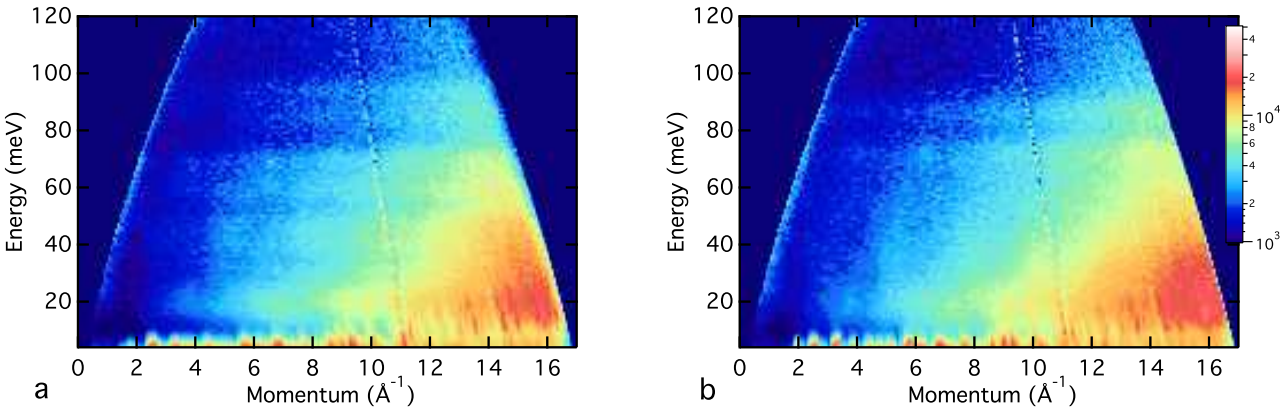

FIG. 1. Intensity of $\chi''(Q, E)$ for (**a**) zirconia and (**b**) 8 mol% YSZ at 300 K from the time-of-flight inelastic neutron scattering measurements with back ground subtracted. The color scales are in log scale, and with the same range. YSZ shows fewer features at low energy transfers.

modes were extremely broad, but curiously, no optical modes were detected.[23]

Here we report results from inelastic neutron scattering measurements on zirconia and YSZ, together with Raman spectrometry measurements of the temperature dependence of specific phonon modes. DFT calculations of the phonons and their Grüneisen parameters are reported for monoclinic and tetragonal zirconia to provide insight into quasiharmonic behavior, where the phonon frequencies depend on temperature only through thermal expansion. Comparisons of calculations to the Raman and neutron measurements show that zirconia and YSZ exhibit substantial anharmonic thermal broadenings and shifts of phonon frequencies that differ from quasiharmonic predictions. The oxygen-dominated modes at higher energies were especially anharmonic. The thermal trends of the phonon peaks are similar in both zirconia and YSZ. In comparison to zirconia, the experimental phonon spectra of YSZ showed substantial broadening at low temperatures, however. The experimental phonon spectrum of YSZ was in some disagreement with the phonon spectrum calculated for the tetragonal structure, unlike the good agreement found for calculation and experiment for monoclinic zirconia. It appears that defects have a significant effect on the phonon spectrum of YSZ. The phonon entropy of YSZ was found to be larger than that of zirconia, as expected for the monoclinic-to-tetragonal phase transition of zirconia at elevated temperature.

II. EXPERIMENTAL

Monoclinic zirconia and 8 mol% YSZ powder (99.99% and 99.95% purity respectively) were loaded into an annular volume between two concentric aluminum cylinders (giving an outer diameter of 2.9 cm, a wall thickness of 1 mm, and a height 6.4 cm), or were loaded into niobium sachets for measurements at higher temperatures. The effective sample thickness for neutron scattering was about 2 mm, giving a ratio of multiple- to single-scattering of approximately 5%. The YSZ sample was characterized by X-ray powder diffraction to be primarily tetragonal, with 8% monoclinic phase. Inelastic neutron scattering measurements were performed with the time-of-flight Fermi chopper spectrometer, ARCS[24], at the Spallation Neutron Source at Oak Ridge National Laboratory. For measurements at 300, 450, 600, and 750 K, the samples were measured in aluminum sample cans inside a low-mass electrical resistance furnace ("stick furnace"). For 300, 673, 1073, and 1373 K, an electrical resistance furnace with niobium radiation shields ("MICAS furnace") was used. Zirconia and YSZ are stable to much higher temperatures, but since small anharmonic effects are linear in temperature, the essential effects of phonon anharmonicity can be determined from the temperatures of these measurements. The incident neutron energies, calculated from experimental data, were 163 meV for measurements with the stick furnace, and 90 and 175 meV for measurements with the MICAS furnace. ARCS has an energy-dependent energy resolution that varied from about 4% at the elastic line to 1% at the highest energy transfer. Temperature was monitored with several thermocouples, and is believed accurate to within 5 K over most of the sample. Furnace backgrounds were measured with empty sample cans at each temperature, and later subtracted from the measurements of the sample.

Data reduction was performed with the software package DRCS[25] for ARCS. For each incident energy, the raw data of individual neutron detection events were first binned to get $S(E, 2\theta)$, where 2θ is the scattering angle and E is the energy transfer, and normalized by the proton current on target. Bad detectors were identified and masked, and the data were corrected for detector efficiency using a white-beam measurement from vanadium. The $S(E, 2\theta)$ was then rebinned into intensity, $S(Q, E)$,

where $\hbar Q$ is the momentum transfer to the sample. The elastic peak was removed and replaced by a function of energy determined from the inelastic scattering just past the elastic peak.[26] Intensities of the imaginary dynamical susceptibility, $\chi''(Q,E) = S(Q,E)/(n_T(E)+1)$, with $n_T(E)$ the Planck distribution, are shown in Fig. 1 for measurements at 300 K. The phonon DOS curves, shown in Fig. 4 and Fig. 5 for the incident energies of 163 or 175 and 90 meV, were obtained after corrections for multiphonon and multiple scattering using the getdos package,[27] as described previously.[26] Neutron diffraction patterns were also obtained by taking elastic scattering cuts. Pair-distribution-functions (PDF) were also calculated using $S(Q)$, as detailed in the Supplemental Materials, and showed overall good agreement with simulations of monoclinic and tetragonal structures. The crystal structure of YSZ remained tetragonal at all temperatures, and that of zirconia remained monoclinic, as expected.

For Raman spectroscopy measurements, samples were mounted on the silver block of a Linkam thermal stage with the chamber sealed and purged with nitrogen gas flow. A temperature controller drove a 200 W power supply for heating the samples for measurements from 300 to 853 K. Raman spectra were measured with a Renishaw micro-Raman system with an Olympus LMPlanFI microscope lens. The spectrometer was configured in backscattering geometry, minimizing issues with the thickness of the sample.[28] A depolarized solid-state laser operated at a wavelength of 514.5 nm excited the sample with the low incident power of 10 mW to avoid additional thermal heating. Each Raman spectrum was accumulated in 20 measurements with 5 s exposure times. The measurements on zirconia were performed on a Raman system described elsewhere,[19,20] but the resolutions of both spectrometers were much narrower than the peaks in the measured Raman spectra and can be safely ignored. The Raman spectra were corrected for background and fitted with multiple Lorentzian peaks to obtain the mean phonon energies and their linewidths.

III. RESULTS

The $\chi''(Q,E)$ results in Fig. 1 show different phonon scattering from zirconia and YSZ at 300 K. The $\chi''(Q,E)$ from YSZ has fewer distinguishable energy-dependent features below 60 meV. The peaks in the measured phonon DOS are broader in YSZ than zirconia at the same temperature. This is consistent with the Raman results shown in Figs. 2 and 3. At 300 K, the linewidths of some Raman peaks of YSZ are up twice as large as the same peaks of ZrO_2. Nevertheless, for both zirconia and YSZ, the Raman peak center energies have similar temperature dependences, and both sets of Raman peaks have similar increases in linewidths with temperature.

Room temperature neutron results from different furnaces were in good agreement after completing data de-

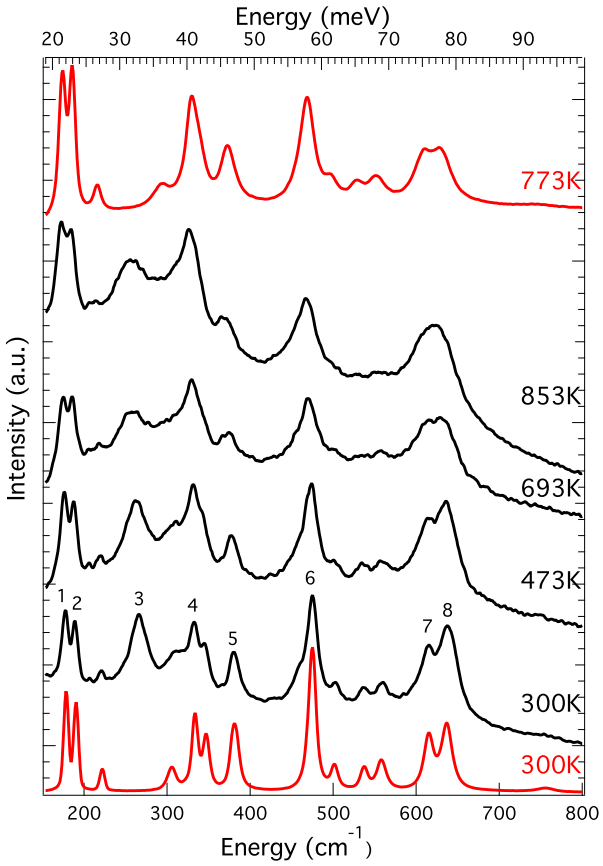

FIG. 2. A comparison of the Raman spectra of zirconia (red, top (773 K) and bottom (300 K)) and YSZ (black) at temperatures as labeled.

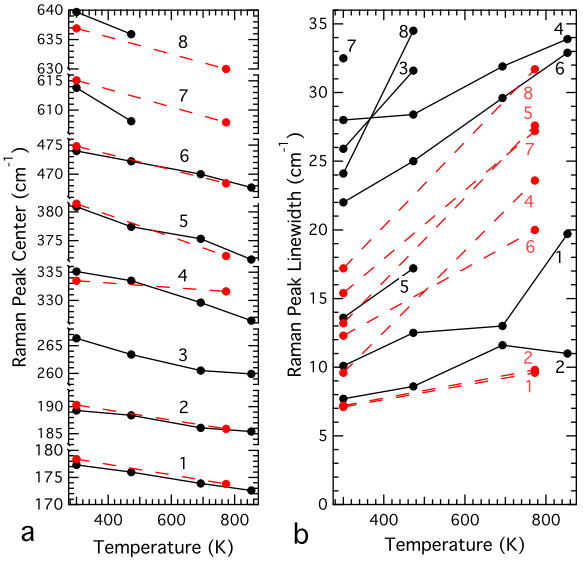

FIG. 3. Temperature dependences of fit parameters for Raman peaks, numbered as in Fig. 2. Solid black lines are for YSZ, and dashed red for ZrO_2. (**a**) Center energy. (**b**) Full-width-at-half-maximum.

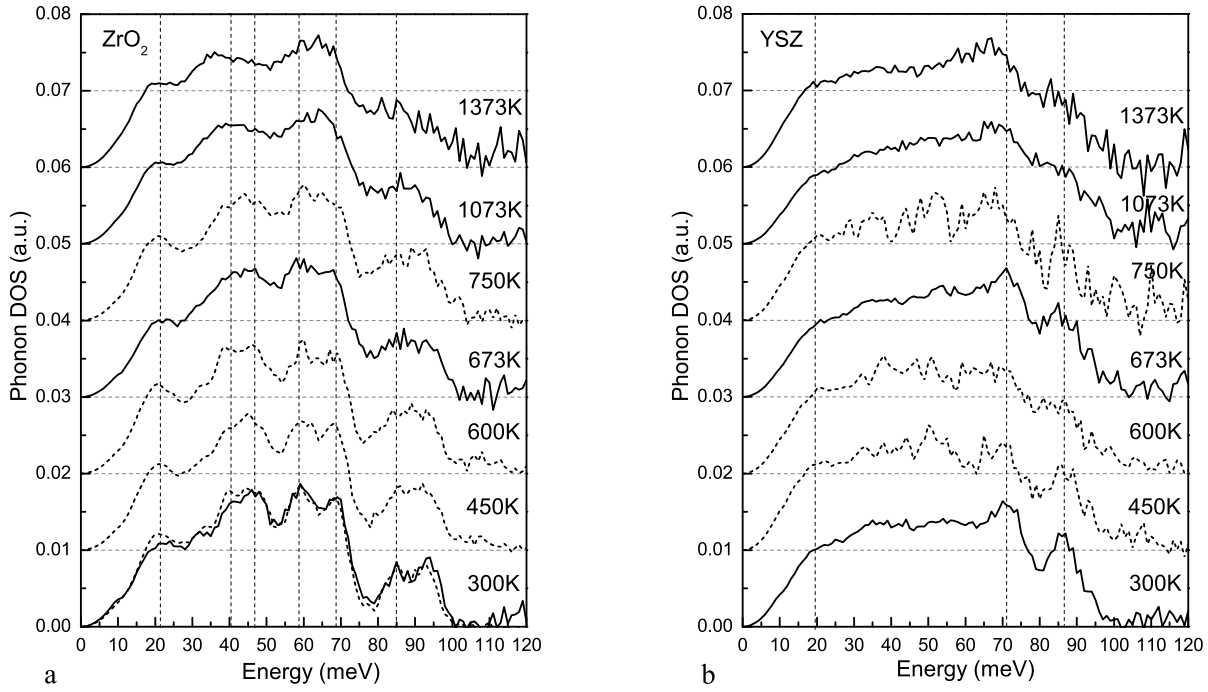

FIG. 4. Normalized neutron-weighted phonon DOS curves of (**a**) zirconia, and (**b**) 8 mol% YSZ from inelastic neutron scattering with 163 or 175 meV incident energies at temperatures from 300 to 1373 K with background subtracted. The solid lines are the results from the MICAS furnace, dashed lines from the stick furnace. The vertical lines are aligned with peaks at 300K.

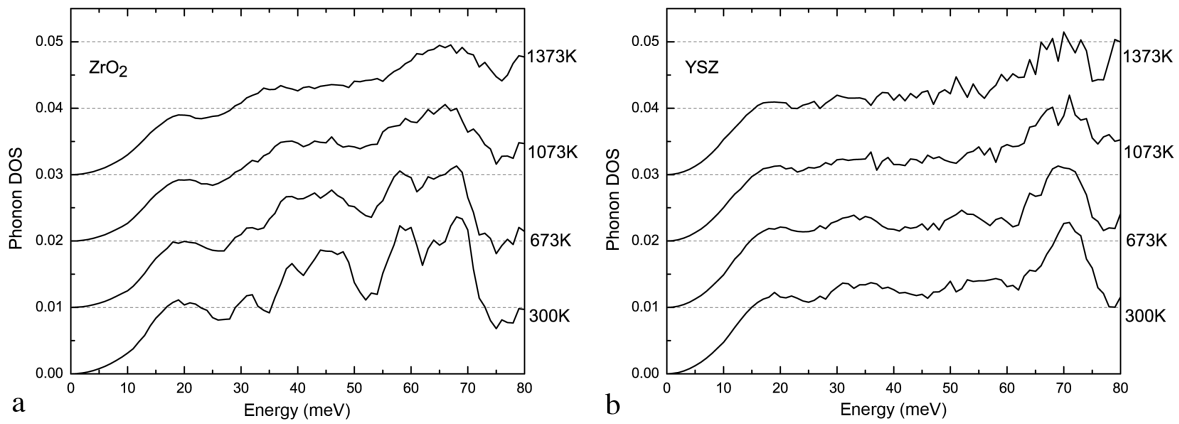

FIG. 5. Neutron-weighted phonon DOS curves of (**a**) zirconia, and (**b**) 8 mol% YSZ from inelastic neutron scattering with 90 meV incident energies at temperatures from 300 to 1373 K in the MICAS furnace with background subtracted. The lower incident energy gives better resolution than the results of Fig. 4.

duction and correcting for the background (Fig. 4). The phonon DOS curves from measurements with an incident energy of 90 meV have higher resolution (Fig. 5), but otherwise are in good agreement with the results in Fig. 4 from higher incident energies. Thermal broadening is the most salient feature of the phonon spectra of zirconia and YSZ measured by both neutron and Raman scattering. Compared to YSZ, the spectra from zirconia have sharper features at low temperatures. Thermal shifts are also apparent, with spectral features from 40 to 80 meV

shifting to lower energies (softening) with temperature.

At about 750 K the phonon modes near 87 meV broaden for both zirconia and YSZ; phonon modes around 70 meV soften and also broaden. The spectra of YSZ are mostly featureless between 20 and 60 meV, even for the higher resolution spectra measured with 90 meV incident energy.

IV. CALCULATIONS

First principles DFT calculations were performed with VASP[29–31], and used to calculate the total and partial phonon DOS curves for pure monoclinic and tetragonal phases. The generalized gradient approximation (GGA) and projector augmented wave (PAW) pseudopotentials were used in all calculations. Electronic structure was calculated self consistently using primitive cell and a $6 \times 6 \times 6$ k-point grid. Experimental lattice parameters[32,33] for ambient conditions of monoclinic zirconia and high-temperature tetragonal phase were used for the calculations. Phonon energies were calculated using the finite displacement method on a $2\times2\times2$ supercell and interpolated to a $16\times16\times16$ k-point grid, which was used to calculated the total and atom-projected phonon DOS. Results for the monoclinic and tetragonal phases are presented in Fig. 6. Figure 6**a** shows that in monoclinic zirconia, the heavier metal-dominated modes are in the low-energy end of the DOS below 40 meV, while the lighter oxygen atoms tend to dominate the high-energy part of the spectrum. This separation is somewhat less strong for the tetragonal phase, as shown in Fig. 6**c**, but again metal-dominated modes are found below 40 meV and the majority of the oxygen-dominated modes are between 40 and 70 meV. This approximate separation into metal modes and oxygen modes is expected from the large difference in the mass of zirconium and oxygen atoms.

For comparison with experimental results, the calculated phonon partial DOS curves of Zr and O were multiplied by σ_{scat}/m, where σ_{scat} is the total cross section for neutron scattering and m is the mass of the atom. (The σ_{scat}/m for Y is nearly the same as for Zr.) Summing these corrected partial DOS curves gave "neutron-weighted" curves for comparison to experiment. Good agreement was found between the experimental DOS for monoclinic zirconia and the neutron-weighted calculation convoluted with the ARCS instrument resolution function, which varies with energy transfer (Fig. 6**b**). The experimental phonon DOS of the YSZ agreed far less well with the calculations for the tetragonal structure. (It is better fit by a mixture of calculated DOS curves, for example 70% tetragonal and 30% monoclinic phase). Some calculated features at energies below 60 meV are conspicuously absent in the experimental spectra from YSZ. Similar calculations for cubic zirconia are shown in Supplemental Materials Fig. 2 and prove that the cubic phase does not produce the neutron results.

Mode Grüneisen parameters

$$\gamma_j = -\frac{V}{\omega_j}\frac{\partial\omega_j}{\partial V} \tag{1}$$

were calculated for modes throughout the Brillouin zone using first-principles and finite displacement methods. The results for monoclinic and tetragonal phases are plotted versus phonon energy in Fig. 7. The inset in Fig. 7 shows that some phonon branches have distinct correlations between γ_j and energy. The monoclinic phase has more negative γ_j than the tetragonal, and a broader distribution. Some mode Grüneisen parameters at low energies are quite large. A large γ_j suggests that the phonon mode is very anharmonic and may not be described reliably by the quasiharmonic approximation.[34]

V. DISCUSSION

A. Quasiharmonicity and Anharmonicity

The temperature dependence of the phonon frequency ω_j can be written as:

$$\frac{\mathrm{d}\omega_j}{\mathrm{d}T} = \left.\frac{\partial\omega_j}{\partial T}\right|_V + \left.\frac{\partial\omega_j}{\partial V}\right|_T \frac{\mathrm{d}V}{\mathrm{d}T} \,. \tag{2}$$

The second term, where the ω_j depends on volume, gives the quasiharmonic softening of a phonon mode owing to thermal expansion

$$\omega_j(T) = \omega_j(0)\exp\left(-\gamma_j \int_0^T \beta(T)\,\mathrm{d}T\right) \,, \tag{3}$$

where β is the volume thermal expansivity and γ_j was defined in Eq. 1.

In a test of the quasiharmonic contributions to the thermal shift of phonon DOS curves, Grüneisen parameters calculated using the quasiharmonic approximation (as shown in Fig. 7), and experimental thermal expansion data[35,36] were used to predict how the phonon DOS should evolve with temperature. The phonon DOS curves measured at 300 K were binned into histograms of 1 meV intervals. For each mode in the interval, its Grüneisen parameter was assessed, and with the thermal expansion the intensity from this mode was shifted to another energy bin. This procedure was repeated for all modes, and the redistributed intensity gave a new DOS from the QHA and mode Grüneisen parameters. The results are compared with the measured phonon DOS curves in Fig. 8. For the monoclinic zirconia the agreement with the experimental DOS curve at high temperature is moderately good, considering that the QHA does not account for any increase in phonon linewidth with temperature. The softening of the spectral feature near 40 meV for monoclinic zirconia is underestimated, however. The agreement is less good for the YSZ, using either the Grüneisen parameters calculated for the

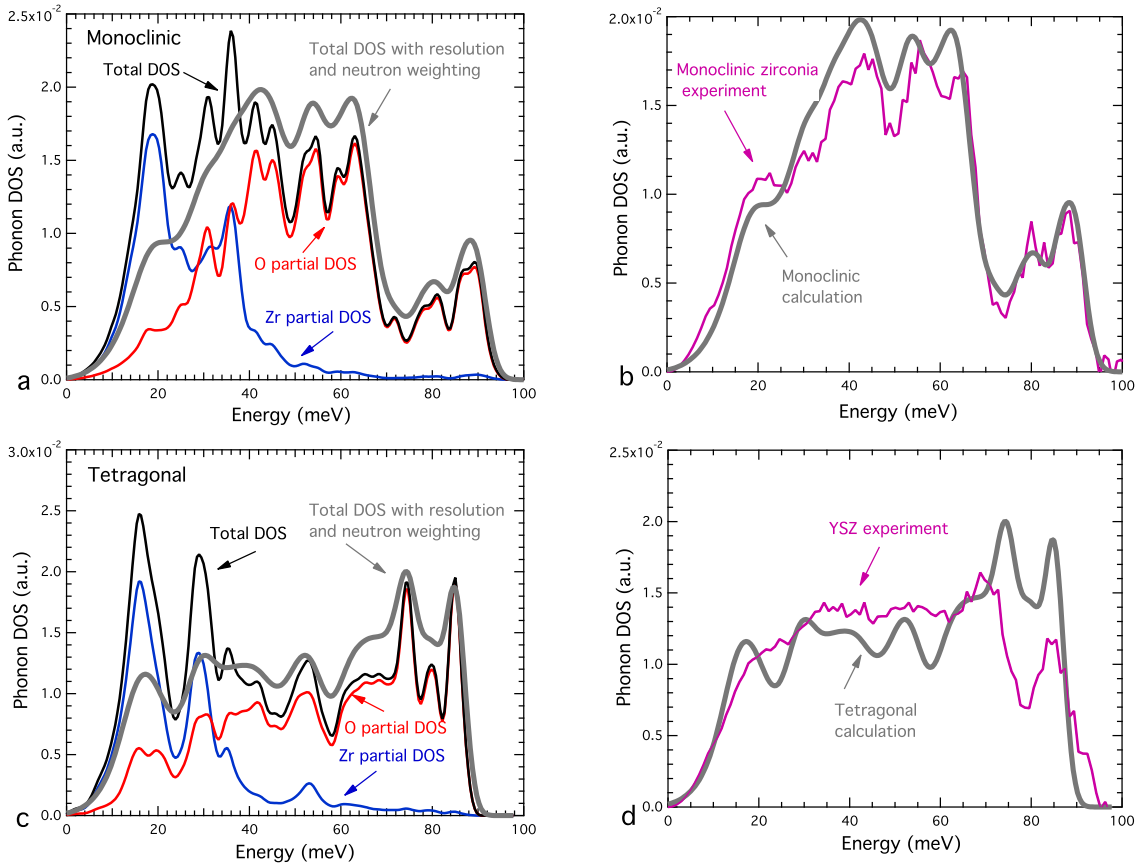

FIG. 6. Total and partial phonon DOS curves of (**a**) monoclinic, (**c**) tetragonal phases from first principles DFT calculations. The thick gray lines are the phonon DOS with proper neutron weighting and ARCS instrument resolution at 163 meV incident energy. They are compared with the results from neutron experiments on monoclinic zirconia (**b**), on YSZ (**d**) at 300 K on the right.

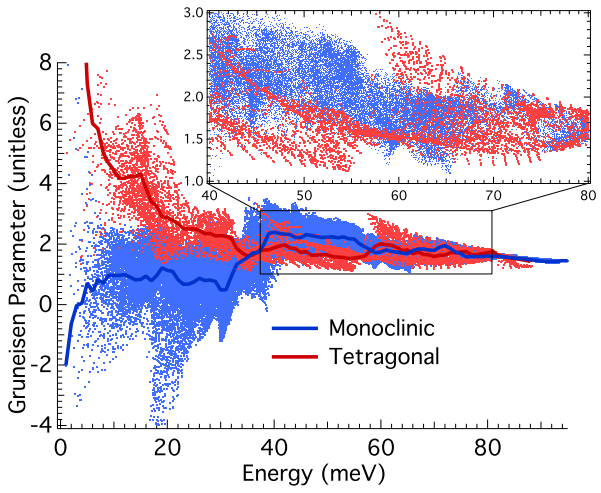

FIG. 7. Grüneisen parameters for monoclinic and tetragonal phases calculated from first-principles and finite displacement methods. The energy-dependent averages are shown as solid lines.

monoclinic phase or the tetragonal phase. Neglecting thermal changes of specific features, the quasiharmonic approximation was reasonably successful for the metal-dominated low-energy modes. The oxygen-dominated high-energy modes were not well described by the QHA. This is consistent with the significant thermal broadening of this part of the spectra, indicative of anharmonicity.

B. Thermal Broadening

At low temperatures, the phonon DOS and Raman spectra of YSZ are broader than in the pure zirconia, especially at lower energies. This probably originates with a distribution of phonon frequencies caused by vacancies and other structural disorder in the YSZ. It could be related to the low thermal conductivity of YSZ at low temperatures. Nevertheless, the high-energy parts of the phonon DOS, dominated by oxygen atom motions, are rather similar in the two materials. With increasing temperature, there is a similar broadening and shift of the two peaks in the phonon DOS curves of zirconia and YSZ at approximately 70 and 85 meV.

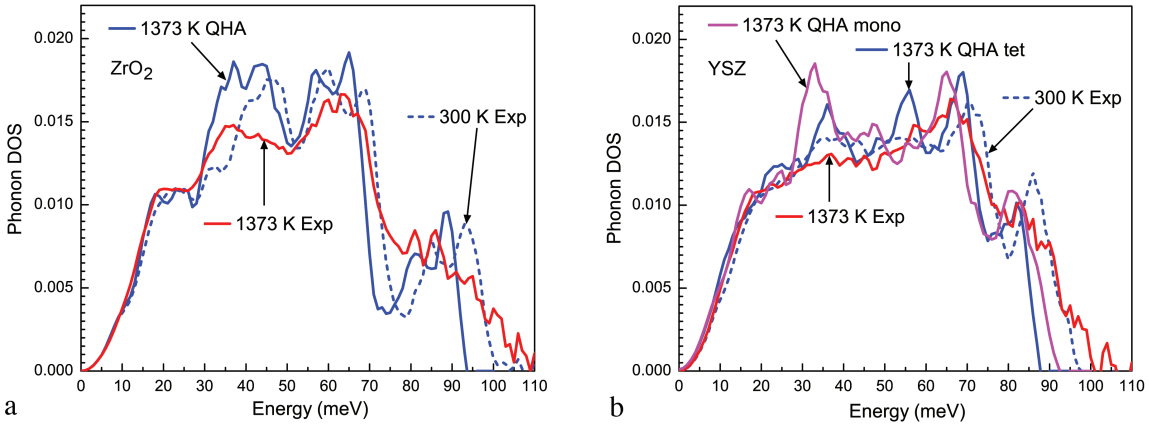

FIG. 8. Experimental phonon DOS curves of (**a**) monoclinic zirconia, and (**b**) tetragonal YSZ compared with the QHA model calculations described in the text. Predictions with mode Grüneisen parameters for both the monoclinic and tetragonal materials are shown in panel b.

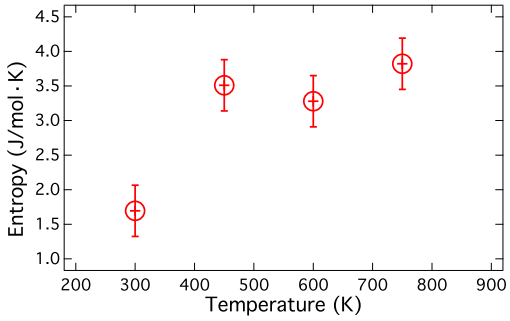

FIG. 9. The approximate difference between phonon entropies of YSZ and monoclinic zirconia, $\Delta S = S_{\rm YSZ} - S_{\rm mono}$, corrected approximately for neutron-weighting.

The Raman spectra of YSZ and zirconia, although limited to phonons at the Γ-point, do show considerable thermal broadening that provides further information about anharmonicity.[37,38] A quasiharmonic analysis cannot, of course, account for linewidth broadening of phonons at elevated temperatures. Anharmonic phonon perturbation theory shows that the leading term in phonon lifetime broadening originates from the cubic anharmonicity[39,40]. The cubic anharmonicity may be especially large in monoclinic zirconia because its atoms do not have inversion symmetry, so it is possible for some phonons to have an odd-order terms in their potential energy. The YSZ shows similar thermal broadening of Raman lines to those of zirconia that we reported recently,[20] although YSZ also has broad linewidths at low temperatures.

C. Phonon Entropy

The entropy of zirconia originates primarily from phonons, which can be described as a sum of harmonic, quasiharmonic, and anharmonic contributions

$$S_{\rm ph} = S_{\rm harm} + \Delta S_{\rm qh} + \Delta S_{\rm anh} \ . \qquad (4)$$

The harmonic contribution, which is the largest, originates with phonons that undergo no change in frequency with changes in either temperature or volume. The Planck occupancy of harmonic phonon modes increases with temperature, giving an increased entropy. The quasiharmonic and anharmonic contributions to entropy can be separated by their dependence on volume and on temperature

$$\frac{{\rm d}S(T,V)}{{\rm d}T} = \left.\frac{\partial S}{\partial T}\right|_V + \left.\frac{\partial S}{\partial V}\right|_T \frac{{\rm d}V}{{\rm d}T} \ . \qquad (5)$$

After accounting for the Planck occupancy change of harmonic phonons, the remainder of the first term on the right of Eq. 5 is the anharmonic contribution, and the second term is the quasiharmonic. Using calculated Grüneisen parameters to describe the frequency change with temperature, the quasiharmonic contribution was approximately successful for phonons in zirconia with energies below about 50 meV, correctly predicting the smaller shift for the feature around 20 meV. On the other hand, the quasiharmonic calculations predicted a distinct softening of spectral features between 50 and 70 meV, and between 80 and 100 meV, but these features stiffened and remained unchanged with temperature, respectively. It appears that the oxygen-dominated modes in zirconia are more anharmonic than the metal-dominated modes, as indicated from previous Raman spectroscopy results.[20] This may originate with the larger average displacements of oxygen atoms than zirconium atoms in higher-energy phonon modes, as expected from the large difference in atomic mass.

The only material parameter needed to calculate the phonon entropy is the phonon DOS, $g(\epsilon)$

$$S_{\rm ph}(T) = 3k_{\rm B}\int_0^\infty g_T(\varepsilon) \Big(\big[\, n(\varepsilon)+1\big] \ln\big[n(\varepsilon)+1\big] - \; n(\varepsilon)\ln\big[n(\varepsilon)\big] \Big)\, {\rm d}\varepsilon \;, (6)$$

where $n(\epsilon)$ is the Planck distribution for phonon occupancy at temperature T. Equation 6 is reliable for the harmonic, quasiharmonic, and anharmonic entropy (approximately), if $g_T(\varepsilon)$ is the phonon DOS at the temperature of interest. Unfortunately, our experimental phonon DOS curves are "neutron-weighted" because phonon scattering by different elements with different efficiencies, proportional to their neutron scattering cross section divided by atomic mass. To determine the absolute entropies of zirconia and YSZ, the neutron weighting was corrected by the calculated partial DOS of monoclinic and tetragonal zirconia, respectively. (The neutron weight correction was largely insensitive to the choice of structure and the details of the DFT calculation.) The difference in phonon entropy between YSZ and monoclinic zirconia is shown in Fig. 9. (For comparing entropies, we selected the low background measurements performed with the low-mass sample and the low-mass stick furnace, for which we had four pairs of measurements.)

Figure 9 shows that monoclinic zirconia has a smaller phonon entropy than YSZ by 1.7 to 3.9 J/mol K (0.28 to 0.65 $k_{\rm B}$/atom) between 300 and 800 K. From the relationship $\Delta S_{\rm qh} = Bv\beta^2 T$ (B is bulk modulus, v is specific volume, β is the coefficient of volume thermal expansion)[8], which is consistent with the phonon entropy if zirconia is a quasiharmonic solid, the bulk properties of zirconia[35] give $\Delta S_{\rm qh} = 0.19\, k_{\rm B}$/atom over a temperature change of 1000 K. In the high temperature limit, this corresponds to an average decrease in phonon frequencies of approximately 6 % in a temperature range of 1000 K if $\Delta S_{\rm qh} = -3k_{\rm B}\ln\langle\omega/\omega_0\rangle$ (where $\langle\omega/\omega_0\rangle$ is an average ratio of phonon frequency at high temperature to that at low temperature). The actual decrease of phonon frequencies is smaller than this, apparently because the anharmonicity in the oxygen-dominated modes causes less thermal softening than predicted by the QHA. Interestingly, we found that using the phonon DOS curves for zirconia and YSZ measured at 300 K with Eq. 6 at elevated temperatures gave similar results to Fig. 9. Even though individual phonons stiffen or soften with temperature quite differently, the overall effects of quasiharmonicity and anharmonicity are similar for both materials, so surprisingly, the difference in phonon entropy of both materials can be obtained approximately from a harmonic model.

For comparison, the difference in vibrational entropy of monoclinic and tetragonal zirconia was also evaluated from the DFT calculations of the phonon spectra at $T = 0$ K. The tetragonal zirconia had the larger vibrational entropy, but the difference in vibrational entropy was only 0.38 J/(mol·K) at 300 K. This suggests that the difference in vibrational entropy between zirconia and YSZ may not arise from the difference in phonon spectra of perfect monoclinic and tetragonal structures. Defects in the YSZ appear to be important.

A recent study by differential scanning calorimetry on the monoclinic-tetragonal phase transition in ZrO_2 gave an entropy of this transition of approximately 3.7 J/(mol·K) at the transition temperature of 1472 K.[41] Although the materials and temperatures are different from the present study, the results of Fig. 9 are consistent in sign and approximately the right magnitude to suggest that much of the entropy of the monoclinic-tetragonal transition originates from changes in the phonon spectra.

VI. CONCLUSIONS

A comparison was made of phonons in monoclinic zirconia (ZrO_2) and 8 mol% yttrium-stabilized tetragonal zirconia (YSZ) from ambient temperature to 1373 K, measured by inelastic neutron scattering spectrometry, Raman spectrometry, and calculated by density functional theory (DFT). Mode Grüneisen parameters were computed by DFT methods, and used to rescale the low-temperature phonon spectrum to predict spectra at high temperatures. This quasiharmonic approximation was reasonably successful for the metal-dominated phonon modes at low energies, but less successful for the oxygen-dominated phonon modes at the higher energies in the spectrum. The Raman peak centers and linewidth broadenings have similar changes with temperature for both zirconia and YSZ. There is substantial anharmonicity in the phonons of both zirconia and YSZ, especially for the oxygen-dominated modes at higher energies. In addition, the phonon spectra of YSZ are broadened significantly at low temperatures, likely due to structural disorder that would also reduce the quality of agreement between computed and experimental phonon spectra of tetragonal YSZ, compared to the good agreement for monoclinic zirconia. At all temperatures, YSZ had a larger vibrational entropy than zirconia.

ACKNOWLEDGMENTS

We thank G.R. Rossman for his generous help on the Raman measurements. This work was supported by the Department of Energy Office of Science through BES Grant No. DE-FG02-03ER46055. The research at Oak Ridge National Laboratory's Spallation Neutron Source was sponsored by the Scientific User Facilities Division, Office of Basic Energy Sciences, DOE.

* lichen@caltech.edu

[1] Q. E. Pierre, P. Barbéris, A. P. Mirgorodsky, and T. Merle-Méjean, J. Am. Ceram. Soc. **85**, 1745 (2002).
[2] R. Ruh and P. W. R. Corfield, J. Am. Ceram. Soc. **53**, 126 (1970).
[3] G. D. Wilk, R. M. Wallace, and J. M. Anthony, J. Appl. Phys **89**, 5243 (2001).
[4] E. P. Gusev, E. Cartier, D. A. Buchanan, M. Gribelyuk, M. Copel, H. Okorn-Schmidt, and C. D'Emic, Microelectron. Eng. **59**, 341 (2001).
[5] C. León, M. L. Lucía, and J. Santamaría, Physical Review B **55**, 882 (1997).
[6] J. Wang, H. P. Li, and R. Stevens, J. Mater. Sci. **27**, 5397 (1992).
[7] K. W. Schlichting, N. P. Padture, and P. G. Klemens, Journal of Materials Science **36**, 3003 (2001).
[8] B. Fultz, Prog. Mater Sci. **55**, 247 (2010).
[9] G. Morell, W. Pérez, E. Ching-Prado, and R. S. Katiyar, Phys. Rev. B **53**, 5388 (1996).
[10] X. Tang and J. Dong, Proc. Natl. Acad. Sci. **107(10)**, 4539 (2010).
[11] T. Lan, C. W. Li, J. L. Niedziela, H. Smith, D. L. Abernathy, G. R. Rossman, and B. Fultz, Phys. Rev. B **89**, 054306 (2014).
[12] P. P. Bose, R. Mittal, N. Choudhury, and S. L. Chaplot, PRAMANA-J Phys **71**, 1141 (2008).
[13] X. Zhao and D. Vanderbilt, Phys. Rev. B **65**, 233106 (2002).
[14] A. A. Demkov, Phys. Stat. Sol. (b) **226**, 57 (2001).
[15] C. Wang, M. Zinkevich, and F. Aldinger, J. Am. Ceram. Soc. **89**, 3751 (2006).
[16] A. Jayaraman, S. Y. Wang, S. K. Sharma, and L. C. Ming, Phys. Rev. B **48**, 9205 (1993).
[17] G. A. Kourouklis and E. Liarokapis, J. Am. Ceram. Soc. **74**, 502 (1991).
[18] C. Li and M. Li, J. Raman Spectrosc. **33**, 301 (2002).
[19] C. W. Li, M. M. McKerns, and B. Fultz, Phys. Rev B **80**, 054304 (2009).
[20] C. W. Li, M. M. McKerns, and B. Fultz, J. Am. Ceram. Soc. **94**, 224 (2011).
[21] V. Lughi and D. R. Clarke, J. Appl. Phys. **101**, 053524 (2007).
[22] E. Kisi and M. Yuxiang, Journal of Physics: Condensed Matter **10**, 3823 (1998).
[23] D. W. Liu, C. H. Perry, A. A. Feinberg, and R. Currat, Phys. Rev. B **36**, 9212 (1987).
[24] D. L. Abernathy, M. B. Stone, M. J. Loguillo, M. S. Lucas, O. Delaire, X. Tang, J. Y. Y. Lin, and B. Fultz, Review of Scientific Instruments **83**, 015114 (2012).
[25] DRCS, http://danse.us/trac/DrChops.
[26] M. Kresch, M. Lucas, O. Delaire, J. Y. Lin, and B. Fultz, Phys. Rev. B **77**, 024301 (2008).
[27] getdos, http://code.google.com/p/getdos/.
[28] T. Lan, C. W. Li, and B. Fultz, Phys. Rev. B **86**, 134302 (2012).
[29] G. Kresse and J. Furthmüller, Comput. Mater. Sci. **6**, 15 (1996).
[30] G. Kresse and J. J. Hafner, Phys. Rev. B **47**, 558 (1993).
[31] G. Kresse and J. Furthmüller, Phys. Rev. B **54**, 11169 (1996).
[32] M. Winterer, R. Delaplane, and R. McGreevy, J. Appl. Crystallogr. **35**, 434 (2002).
[33] D. G. Lamas and N. E. Walsöe De Reca, International Journal of Thermophysics **35**, 5563 (2000).
[34] C. W. Li, X. Tang, J. A. Munoz, J. B. Keith, S. J. Tracy, D. L. Abernathy, and B. Fultz, Phys. Rev. Lett. **107**, 195504 (2011).
[35] Y. S. Touloukian, Thermophysical Properties of High Temperature Solid Materials, Vol. 4 (1966).
[36] H. Hayashi, T. Saitou, N. Maruyama, H. Inaba, K. Kawamura, and M. Mori, Solid State Ionics **176**, 613 (2005).
[37] J. Serrano, F. J. Manjón, A. H. Romero, F. Widulle, R. Lauck, and M. Cardona, Phys. Rev. Lett. **90**, 055510 (2003).
[38] J. Serrano, F. Widulle, A. Romero, A. Rubio, R. Lauck, and M. Cardona, Phys. Stat. Sol. (b) **235**, 260 (2003).
[39] D. Wallace, Thermodynamics of Crystals (Wiley, New York, 1972).
[40] A. A. Maradudin, A. E. Fein, and G. H. Vineyard, Phys. Stat. Sol. (b) **2**, 1479 (1962).
[41] Y. Moriya and A. Navrotsky, J. Chem. Thermodyn. **38**, 211 (2006).